Amorphous binary dispersions of chloramphenicol in enantiomeric pure and racemic poly-lactic acid: morphology, molecular relaxations, and controlled drug release

Sofia Valenti,[1,2] Angelica Diaz,[2,3] Michela Romanini,[1,2,†] Luis Javier del Valle,[3] Jordi Puiggalí,[2,3] Josep Lluis Tamarit,[1,2] and Roberto Macovez [1,2,]*

[1] Grup de Caracterització de Materials, Departament de Física, Universitat Politècnica de Catalunya, EEBE, Av. Eduard Maristany 10-14, E-08019 Barcelona, Spain.

[2] Barcelona Research Center in Multiscale Science and Engineering, Universitat Politècnica de Catalunya, Campus Diagonal-Besòs, Av. Eduard Maristany 10-14, E-08019 Barcelona, Spain.

[3] Synthetic Polymers: Structure and Properties. Biodegradable Polymers, Departament de Enginyeria Química, Universitat Politècnica de Catalunya, EEBE, Av. Eduard Maristany 10-14, E-08019 Barcelona, Spain.

* Corresponding author. Electronic mail: roberto.macovez@upc.edu.

† Current address: Departament de Física de la Matèria Condensada, Facultat de Física, Av. Martí i Franquès 1, E-08028 Barcelona, Spain.

KEYWORDS: Amorphous drug, polymer enantiomerism, molecular mobility, plasticizer dielectric spectroscopy, controlled liberation.

ABSTRACT

We study amorphous solid dispersions (ASDs) of the chloramphenicol antibiotic in two biodegradable polylactic acid polymers, namely a commercial sample of enantiomeric pure PLLA and a home-synthesized PDLLA copolymer, to study the effect of polylactic acid in stabilizing the amorphous form of the drug and controlling its release (*e.g.* for antitumoral purposes). We employ broadband dielectric spectroscopy and differential scanning calorimetry to study the homogeneity, glass transition temperature and relaxation dynamics of solvent-casted ASD membranes with different drug concentrations. We observe improved physical stability of the ASDs with respect to the pure drug, as well as a plasticizing effect of the antibiotic on the polymer, well described by the Gordon-Taylor equation. We study the release of the active pharmaceutical ingredient from the films in a simulated body fluid through UV/vis spectroscopy at two different drug concentrations (5 and 20% in weight), and find that the amount of released drug is proportional to the square root of time, with proportionality constant that is almost the same in both dispersions, despite the fact that the relaxation time and thus the viscosity of the two samples at body temperature differ by four orders of magnitude. The drug release kinetics does not display a significant dependence on the drug content in the carrier, and may thus be expected to remain roughly constant during longer release times.

1. Introduction

Most drugs are poorly water-soluble, so that additional strategies must be employed to enhance their bioavailability. (Williams et al., 2013) Of the various possible approaches to enhance the solubility of active pharmaceutical ingredients, amorphization offers the advantage that it does not require chemical modification of the drug. Solid amorphous (glassy) pure drugs have a proven higher effective solubility *in vivo* and better dissolution profiles compared with the crystalline form of the drug. (Murdande et al., 2011; Gupta et al., 2004; Hancock and Parks, 2000; Craig et al., 1999; Serajuddin, 1999) On the other hand, glasses are thermodynamically unstable due to their excess in free energy and enthalpy, and are therefore susceptible to convert into the more stable and less soluble crystalline phase by recrystallization. One of the ways to improve the stability of an amorphous drug is by dispersing it in a biopolymer excipient. (Romanini et al., 2018) There are various methods available to obtain amorphous solid dispersions (ASDs), and in all of them an energy input in the form of heat proves to be beneficial to increase the homogeneity of the dispersion and thus its kinetic stability against recyrstallization. (Dedroog et al., 2019) However, heating can also have drawbacks, especially for drugs that are not thermally stable.

Among biodegradable polymers, polylactic acid has been extensively studied and used in pharmacology as excipient in solid dispersions with active pharmaceutical ingredients, thanks also to its mechanical properties which allow its implementation in sutures, microspheres, scaffolds, and other drug delivery systems. (Abulateefeh et al., 2019;

Jelonek et al., 2019; Llorens et al., 2014; Jain et al., 2013; Llorens et al., 2013; Zheng et al., 2010; Bourges et al., 2003; Soriano et al., 1996) The monomer of polylactic acid exists in two enantiomeric forms, namely, L- and D- lactic acid. The properties of polylactic acid samples depend on the distribution of chiral units in the chains, which in particular determines the capacity of the polymer to crystallize. For example, poly-L-lactic acid (PLLA) synthesized by ring opening of enantiomer-pure L-lactic acid is semicrystalline with a glass transition temperature T_g = 332 K and a melting point T_m = 443 K, while poly-(D,L)-lactic acid (PDLLA) synthesized from the racemic mixture of L and D enantiomers is totally amorphous (T_g can vary between 323 and 329 K depending on molecular weight and polydispersion) due to the intrinsic disorder introduced by the different tacticity (chirality) of its monomers. The purpose of the present paper is to study the impact of the enantiomeric form of polylactic acid on the physical properties of polymer dispersions of the chloramphenicol antibiotic, by comparing dispersions obtained in both PLLA and PDLLA.

The hydrophobicity of polylactic acid can be exploited for the design of controlled release medicaments. Controlled release aims to increase the drug's therapeutic activity and reduce its side effects, as the number of required administrations decreases. This is particularly important in cancer therapies that employ anticancer agents that do not attack only tumor cells, and whose unspecificity together with high dosages leads to serious side effects. (Kalaydina et al., 2018; Senapati et al., 2018; Dang et al., 1994) Chloramphenicol (CAP) is a broad-spectrum antibiotic used for the treatment of a number of bacterial

infections. It blocks protein growth, inhibiting peptide bond formation by binding to a peptidyl transferase enzyme of the bacterial ribosome; thanks to this general mechanism, it proved effective against Gram-positive as well as Gram-negative (e.g. rickettsiae) bacteria. (Monro and Vazquez, 1967) Although it had previously fallen into disuse due to limitations on the amount that can be applied not to cause systemic toxicity, CAP has become an alternative to treat multi-drug-resistant bacteria and has been recently suggested as a potential anticancer drug. (Rivas et al., 2018; Tian et al., 2016; Kostopoulou et al., 2014)

We have shown in a recent article that CAP is prone to degradation at high temperatures. (Valenti et al., 2018) In particular, we found that exposure of the drug to humid atmosphere and subsequent heating to its melting point (T_m = 423 K) (O'Neil, 2013; Ford, 1987) degrades the compound, something that should be avoided due to the possible toxicity of degradation products. The motivation for the present work is twofold: on one hand, devising an optimum temperature range for obtaining ASDs of active pharmaceutical ingredients, which should favor the dispersion's homogeneity while not compromising the chemical stability of the drug; on the other hand, investigating possible benefits of using an intrinsically amorphous polymer, rather than a semicrystalline one, for ASDs. We have chosen a test system with a high potential medical impact, namely, ASDs of a novel antitumoral agent in a biodegradable polymer excipient. Thermal aspects are important for ASDs in polylactic acid because, even though cold crystallization of the enantiomeric pure forms of polylactic acid does not take place until

~373 K, temperature fluctuations may hinder the stability of ASDs with these polymers also at lower *T*.

We show that amorphous PDLLA offers the advantage of a lower temperature of preparation of solvent-free amorphous dispersions and the lack of crystalline polymer fraction, which avoids macroscopic phase separation. The lower temperature is due to the fact that the solvent required for swelling and dissolving polylactic acid, chloroform, remains trapped in the polymer matrix and heating to above 380 K is needed to achieve complete evaporation of this toxic solvent. Solvent evaporation at this temperature triggers however the cold crystallization of PLLA, which means that a further treatment to melt the sample is needed to obtain fully amorphous samples. Using PDLLA, amorphous samples are instead obtained immediately after solvent evaporation. In this case cold crystallization is prevented due to the random disposition of L and D units and consequently problems related to subsequent heating can be avoided. On the drawback side, however, we find that the ASDs in PDLLA are less homogeneous on the molecular scale than fully amorphous dispersions in PLLA. We argue that this occurs because of the intrinsic disorder of the racemic polymer, and thus larger free volume available for molecular motions; this results not only in a lower glass transition temperature of PDLLA compared to PLLA, as experimentally observed, but also in larger local voids where nanoscopic domains of pure amorphous CAP are more likely to form, resulting in a more heterogeneous structure on the molecular level.

These results indicate that the choice of a fully amorphous (random) polymer is not necessarily better than a polycrystalline one to obtain stable and homogeneous ASDs. In

either case, fully dispersed CAP molecules and nanoscopic amorphous domains of CAP trapped in the polymer matrix are advantageous for drug release applications, compared to the crystalline form of the drug. By characterizing the release of CAP from PDLLA membranes with two different drug concentrations (containing 5 and 20% of drug in weight), we show that the antibiotic is released slowly in a Simulated Body Fluid at human body temperature, with released concentration proportional to the square root of time, as predicted both by Fickian diffusion in a thin polymer sample and by the Higuchi model. The proportionality constant differs by a small factor of the order of unity in both dispersions. Interestingly, the release kinetics is roughly the same in the 5% and 20% despite the fact that the relaxation time and thus the viscosity of the two samples at body temperature differ by a factor of 10^4, due to the plasticizing effect of the drug on the polymer, which is more prominent at higher drug content. The fact that the drug release kinetics is only weakly dependent on drug content is beneficial as it allows maintaining a steady release rate as the polymer carrier unloads.

2. Materials and methods

Chloramphenicol ($C_{11}H_{12}Cl_2N_2O_5$, M_w = 323.13 g/mol) was purchased from Sigma-Aldrich with a purity higher than 98%. PLLA grade 4032D, a semi-crystalline material with a concentration of D enantiomers less than 2%, was purchased from Natureworks LLC, USA. L-lactide, with a purity higher than 98% and the 50:50 racemic mixture of D-,L-lactide, with a purity higher than 99%, were purchased by Sigma Aldrich and stored in a fridge at 4 ºC. PDLLA was synthesized in our lab by melt-ring open

polymerization of D-, L-lactide in nitrogen atmosphere at 140 ºC for 24 h. Stannus octanoate was used as an initiator of the reaction. The resulting polymer was dissolved in dichloromethane and precipitated in methanol. It was then filtered with a Buchner funnel and dried in a vacuum oven at ambient temperature for 48 h. The molecular weight (M_w) and polydispersity index (PDI) were assessed by means of gel permeation chromatography using poly(methyl methacrylate) standards. Molecular weights were estimated by size exclusion chromatography (GPC) using a liquid chromatograph (Shimadzu, model LC-8A) equipped with an Empower computer program (Waters). A PL HFIP gel column (Polymer Lab) and a refractive index detector (Shimadzu RID-10A) were employed. The polymer was dissolved and eluted in 1,1,1,3,3,3-hexafluoroisopropanol at a flow rate of 1 mL/min (injected volume 100 μL, sample concentration 2.0 mg/mL). The number and weight average molecular weights were calculated using poly(methyl methacrylate) standards. The synthesized PDLLA had M_w = 53759 g/mol and PDI = 2.68. The chemical composition of the polymer was ascertained by infrared and NMR spectroscopy: the results can be found in the Supplementary Information.

Binary mixtures of CAP with polylactic acid were obtained by dissolving PLA in chloroform in a magnetic stirrer at 310 K for more than a day. The correct amount of CAP to achieve a desired drug loading was dissolved in acetone and the solution was then added to the PLA/chloroform mixture. Films were prepared by solvent casting directly on the desired supports, followed by heating to 393 K (PDLLA) or to 433 K

(PLLA) to allow all solvents to evaporate and to melt the crystalline fraction formed during solvent evaporation in the case of PLLA. Five different concentrations (5, 10, 15, 20 and 30 % wt /wt) were prepared with PLLA, and three with PDLLA (5, 10, 20 % wt/wt).

Differential scanning calorimetry (DSC) experiments were carried out in open aluminum pans under nitrogen atmosphere, by means of a Q100 calorimeter from TA Instruments. Measurements were performed with a heating/cooling rate of 10 K/min and sample mass around 10 mg. A Novocontrol Alpha analyzer was used for broadband dielectric spectroscopy (BDS) measurements. The sample was placed in a stainless steel parallel-plate capacitor specially designed for the analysis of liquid samples, with the two electrodes kept at a fixed distance by means of silica spacers of 50 μm diameter. Temperature control of the capacitor and thus of the sample was achieved with a nitrogen-gas flow cryostat with an error not higher than 0.1 K. The solvent-casted films were heated to 393 (PDLLA) or 433 (PLLA) K prior to measurement to eliminate any remaining solvent. The sample was then rapidly cooled to 133 K and isothermal spectra were then acquired by increasing the temperature in a stepwise fashion, waiting each time 5 minutes for temperature stabilization. Spectra were acquired in the frequency (ν) range between 10^{-2} and 10^{6} Hz.

To obtain relaxation times and quantify the changes in relaxation dynamics, we fitted the dielectric spectra (real and imaginary part simultaneously) as the sum of a power law representing the dc conductivity contribution and a Havriliak-Negami function for each

relaxation component. The analytical expression of the Havriliak-Negami function is (Havriliak and Negami, 1967):

$$(1)\ \varepsilon^*(\omega) = \varepsilon_\infty + \frac{\Delta\varepsilon}{(1+(i\omega\tau_{HN})^a)^b}$$

Here $\omega = 2\pi\nu$ is the angular frequency, ε_∞ is the permittivity in the high frequency limit, $\Delta\varepsilon$ is the dielectric intensity or strength, *a* and *b* are parameters describing the shape of the loss curves and τ_{HN} is a time parameter connected to the characteristic relaxation time $\tau_{max,}$ corresponding to the maximum of the relaxation time distribution. In terms of the fit parameters, τ_{max} is given by:

$$(2)\ \tau_{max} = \tau_{HN}\left[\sin\left(\frac{a\pi}{2b+2}\right)\right]^{-1/a}\left[\sin\left(\frac{ab\pi}{2b+2}\right)\right]^{1/a}$$

The shape parameters *a* and *b* can vary between 0 and 1. Specific cases of the HN function are the Cole-Cole (CC) (Cole and Cole, 1942) and Cole-Davidson (CD) (Davidson and Cole, 1951) functions, which are obtained for $b = 1$ and $a = 1$, respectively, and for both of which $\tau_{max} = \tau_{HN}$. The primary structural relaxation of glass forming materials usually displays an asymmetric Havriliak-Negami line shape, while most secondary relaxation components are broad and symmetric, and can often be described with the Cole-Cole function.

The drug release measurements were carried out in a Simulated Body Fluid (SBF), prepared following a published study (Kokubo and Takadama, 2006). ASD films with 5% and 20% weight fraction of CAP were casted on silica glasses of 1 cm diameter.

Three films were studied for both concentrations; they were inserted in dialysis bags which were then immersed in 20 mL of SBF. The so prepared tubes were then left agitating in an orbital shaker at 80 rpm and 37 ºC for one week. Ethanol was added to the solutions after 3 days of agitation, so as to obtain a 70% ethanol - 30% SBF mixture. The 1 mL samples taken from the tubes at different times during agitation, were analyzed by UV spectroscopy using a Shimadzu 3600 Spectrometer. The total amount of loaded drug was then determined by dissolution of the films in pure ethanol.

3. Results and Discussion

3.1. DSC study

Fig. 1(a) displays the DSC thermograms of a PLLA and a PDLLA sample obtained by solvent casting from chloroform solution followed by annealing above the melting temperature of the polymer and subsequent cooling to below room temperature. The glass transition temperature T_g of the racemic PDLLA sample is lower (by about 10 K) than that of the PLLA sample. Since T_g is basically invariant with the chain molecular weight at the molecular mass that we study (Dorgan, 2005), the change of T_g between the two enantiomeric forms is likely to arise from a larger free volume available for chain motion in the PDLLA case compared with the PLLA case, which could result from the fact that the random distribution of monomers of different chirality (twist direction) leads to a slightly lower effective density in the amorphous phase compared to that of the

enantiomeric pure PLLA sample. Unfortunately, available density data on PDLLA and PLLA do not allow a detailed comparison to confirm this hypothesis.

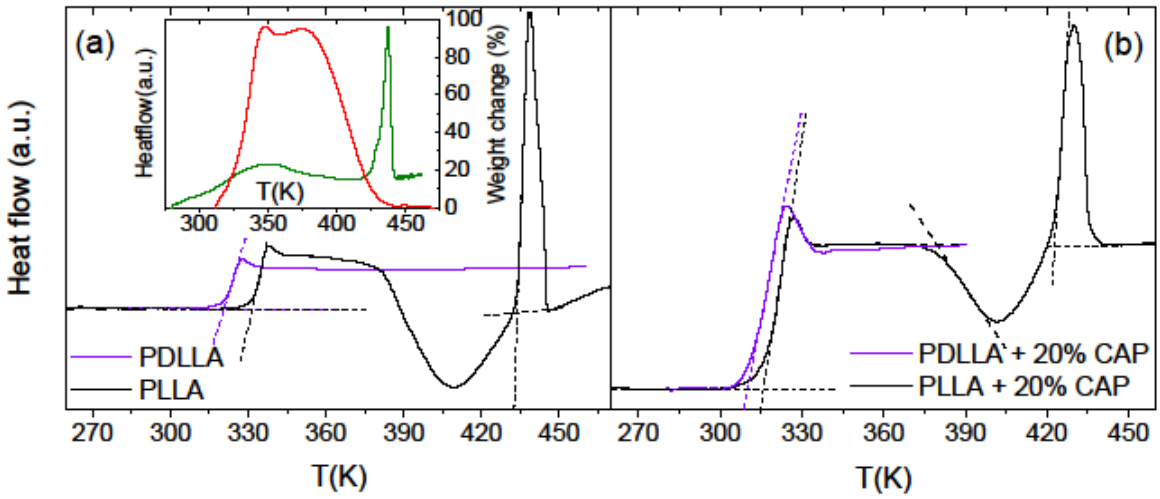

Fig. 1. DSC traces of solution-casted PLLA and PDLLA, both pristine (a) and mixed with 20% CAP in weight (b). Dashed lines indicate the determinations of T_g, T_r and T_m. Inset to (a): DSC thermogram of a PLLA sample (left axis) after solvent casting, where the endotherm corresponding to the loss of the remaining solvent (chloroform) and the melting peak can be observed and TGA traces (right axis) of the same sample, where the maximum of the weight change corresponds to the loss of the remaining chloroform.

It may be observed in the DSC traces that while PLLA cold crystallizes and then melts upon heating, our synthesized PDLLA sample always remains amorphous. The same behavior is also observed in the dispersions with 20% CAP in weight, as shown in Fig. 1(b). It is important to notice that a single T_g value is observed in the thermograms of panel (b), which indicates the lack of macroscopic regions of amorphous phase separation

in the solid dispersions. Four (respectively, five) different concentrations of CAP in PDLLA (resp. PLLA) were studied. Panels (a) and (b) of Fig. 2 display the DSC traces for all the concentrations prepared, including pure CAP (T_g = 300 K). In the PLLA case, the sample with 30% CAP in weight displayed two distinct T_g, both of which lie in between the T_g of the pure components, indicating that this sample is not homogeneous but rather is in a mixed phase. On the other hand, samples with CAP weight fraction of 20% or lower were homogeneous with only a single T_g. We therefore restrict our discussion to samples with up to 20% weight content of CAP.

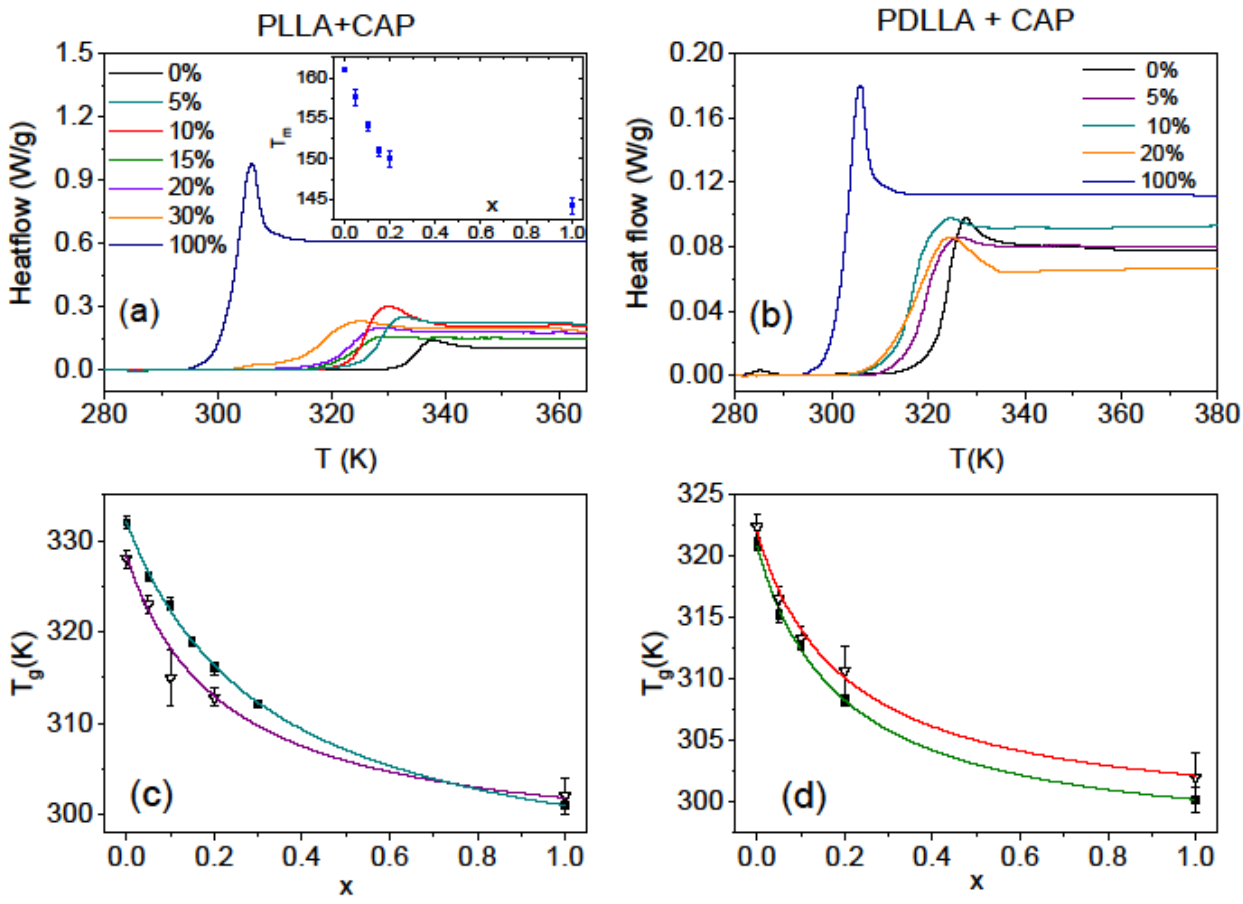

Fig. 2. (a,b) DSC thermograms of the ASDs of CAP in PLLA (a) and in PDLLA (b) around the glass transition temperature, as a function of the drug weight fraction of drug. Inset to (a): melting point of the ASDs with PLLA, as a function of the drug weight fraction. (c,d) Glass transition temperatures of the ASDs of CAP in PLLA and PDLLA, as a function of the drug weight fraction, as obtained by calorimetry (filled markers) and dielectric spectroscopy (open markers, see text for details). Solid lines are fits with the Gordon-Taylor Eq. (3).

In terms of the solubility and reproducibility of a drug formulation, but also of its physical stability, the phase behavior of the PDLLA samples displayed in Fig. 1 is *a priori* preferred (Siepmann et al., 2019), as the lack of a crystalline polymer phase entails that the ASDs cannot phase-separate by formation of lamellae and spherulites of the pure polymer. The resulting macroscopic phase separation is to be avoided, as it implies that a homogeneous drug concentration cannot be guaranteed when the sample is split in smaller portions for administration purposes, and also that the dissolution profile of the drug in the human body may not be uniform in time due to the different swelling of crystalline and amorphous polymer fractions and to the different release time of drug molecules nearer or further from a spherulite. The lack of a macroscopic phase separation is also beneficial as it prevents local overdose and drug toxicity effects.

Although in the DSC traces the recrystallization of the ASDs in PLLA is observed only at a temperature T_{cc} much higher than the storage or even body temperatures, it should be considered that the preparation of the binary mixtures is carried out from a co-dissolution, with the polymer initially dissolved in chloroform, and that an annealing step is required to get rid of the toxic solvent from a bulk polymer sample. Another option would be a method based on the micronization of the sample by spray drying or electrospinning, which we did not employ; however, fast solvent evaporation by means *e.g.* of freeze drying or spray drying could also lead, in general, to formation of small crystalline PLLA domains. As visible in the inset to Fig. 1(a), this annealing step leads to partial crystallization of the PLLA dispersions; therefore, the pure PLLA polymer and CAP dispersions in PLLA need to be annealed again above the melting point of PLLA

(423 K) to obtain a homogeneous amorphous sample. Such a high temperature required to obtain the ASDs with PLLA is not desirable: in general, drug molecules do not withstand annealing to high temperature, and in the specific case of CAP the melting point of PLLA lies above the temperature where hydrated CAP starts degrading, which implies that it cannot be guaranteed that the mixtures do not contain degradation (hydrolysis) products of CAP (Rivas, 2018). Instead, for the PDLLA-CAP mixtures only an annealing step at the desorption temperature of the solvent (380 K) is required. This ensures that our PDLLA-CAP samples are not degraded; this constitutes a second important reason to prefer the amorphous (racemic) PDLLA polymer, rather than PLLA, to obtain solid dispersions of active pharmaceutical ingredients.

Panels (c) and (d) of Fig. 2 exhibit the glass transition temperature (T_g) of ASDs with up to 20% weight fraction of CAP, as obtained from the DSC thermograms shown in panels (a) and (b) of the same figure. For comparison purposes, the so-called dynamic glass transition temperatures for the same samples, obtained by means of dielectric spectroscopy and defined in Section 3.2, are also shown in the lower panels. CAP has a clear plasticizing effect on the polylactide chains, with a substantial reduction of the T_g of the ASDs with respect to the pure polymer. The effect is more dramatic in the PLLA case (Fig. 2(a)) due to the larger difference in T_g between the pure components compared with the PDLLA case (Fig. 2(b)). The continuous lines in Figs. 2(c) and (d) are fits with the Gordon-Taylor equation, given by (Gordon and Taylor, 1952):

(3) $T_{g,ASD} = \frac{(1-x)\,T_{g,PLA} + Kx\,T_{g,CAP}}{1-x+Kx}$,

Here, x is the weight fraction of the drug, $1 - x$ the weight fraction of the polymer, and $T_{g,PLA}$ and $T_{g,CAP}$ are the experimental glass transition temperatures of the pure polymer and pure drug, respectively. The dimensionless constant K is a phenomenological parameter used to account for the curvature observed in the dependence of the T_g of the ASDs with weight fraction. The value of K is found to be 0.24 ± 0.03 and 0.17 ± 0.03 in the case of PLLA and PDLLA, respectively.

The dispersion of CAP into PLLA also leads to a depression of the melting point T_m of pure PLLA, as visible in the inset to Fig. 2(a). The dependence of T_m with drug content has a similar curvature than that of the Gordon-Taylor equation representing the dependence of T_m with drug fraction, as expected due to the rule of thumb according to which T_g should be roughly equal to two thirds the value of T_m. Table 1 summarizes the calorimetric results on the solid amorphous dispersions of CAP in polylactic acid. In the case of the dispersions in PLLA, the recrystallization temperature (T_r) and subsequent melting (T_m) temperatures are included. The recrystallization temperature is defined as the temperature at which the onset of the exothermic recrystallization process is observed in DSC thermograms acquired while heating an initially fully amorphous sample from below T_g at a rate of 10 K min^{-1}. It may be observed from Fig. 2(a) and (b) that the plateau value of the mass-normalized heat flow in the supercooled liquid phase of all homogeneous mixtures (above their T_g) is intermediate between that of the pure polymer and that of pure CAP.

Table 1. Glass transition (T_g), cold crystallization (T_{cc}), and melting (T_m) temperatures for PLLA+CAP and PDLLA+CAP mixtures. T_r and T_m do not exist for PDLLA dispersions as this polymer is amorphous.

Matrix	**CAP wt %**	T_g **DSC [K]**	T_g **BDS [K]**	T_{cc} **[K]**	T_m **[K]**
PLLA	0%	332.4 ± 0.6	328.5 ± 0.2	382.4 ± 0.5	434.2 ± 0.3
PLLA	5%	325.5 ± 0.5	323.0 ± 0.5	388 ± 2	431 ± 1
PLLA	10%	323.3 ± 0.7	315 ± 1	379.0 ± 0.6	427.2 ± 0.6
PLLA	15%	319.1 ± 0.5	-	379.6 ± 0.8	424.1 ± 0.5
PLLA	20%	317.7 ± 0.7	312.8 ±0.5	375.6 ± 0.8	423.2 ± 0.2
PDLLA	0%	321.0 ± 0.5	320 ± 1	-	-
PDLLA	5%	315.2 ± 0.5	318 ± 2	-	-
PDLLA	10%	312.9 ± 0.2	315 ± 1	-	-
PDLLA	20%	308.3 ± 0.5	311 ± 2	-	-

3.2. BDS study

We turn now to our dielectric results on the binary mixtures. Fig. 3 displays selected dielectric loss spectra of homogeneous dispersions of CAP in both PLLA (panels a and b) and PDLLA (c and d) at different weight fractions of the drug. Each isothermal spectrum is normalized to the height of the main relaxation visible in the experimental frequency range at the measuring temperature. The main loss observed in the high temperature panels a and c (T = 338 K) corresponds to the structural (α) relaxation of the dispersions, whose maximum is visible only above T_g. It is found that, for a given fixed temperature, the characteristic frequency of the α relaxation (peak value) shifts to higher values when the CAP weight fraction increases. The difference in glass transition temperature of PLLA and PDLLA samples is reflected in a different frequency position of the α relaxation at the temperature of 338 K (Fig. 3(a) and (c)). Since a higher relaxation frequency means faster dynamics, the spectra in these panels constitute the frequency-domain observation of the plasticizing effect of CAP on both polymers.

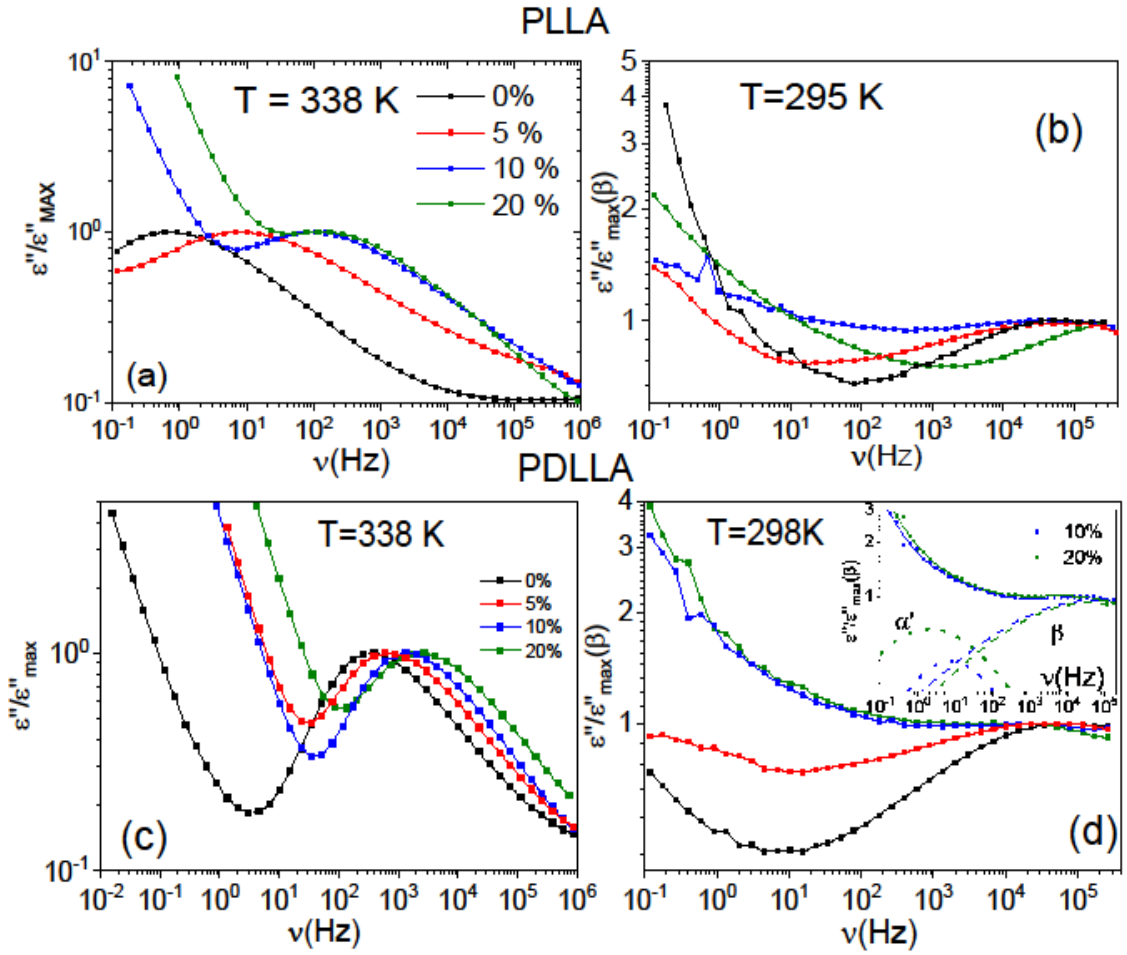

Fig. 3. Normalized dielectric loss spectra of CAP+PLLA (left panels) and CAP+PDLLA (right panels) dispersions with different weight fraction of the drug (see legends) at the fixed temperatures of 338 K, where the structural primary relaxation is visible (a,c), 295 K, where a secondary relaxation is observed in PLLA dispersions (b) and 298 K, where two different relaxations are found in PDLLA dispersions (d). Inset to panel (d): dielectric loss spectra of PDLLA with 10 and 20% drug weight fraction (points). Dotted and dashed lines represent the two different spectral components, while the solid line represents the total fit.

The loss feature observed in the lower-temperature panel (b), peaked between 10 and 100 kHz, corresponds instead to the secondary β relaxation of the polymer (Ren et al., 2003), which is obviously absent in the pure supercooled CAP sample. The same relaxation is observed also in the PDLLA polymer (panel (d)) and in the ASDs of CAP in both polymers. While for pure PDLLA and for the 5% CAP dispersion in the racemic polymer only the α and β relaxations are visible, in the 10% and 20% dispersions in PDLLA a third relaxation feature is observed, absent in other samples, which has a lower intensity (dielectric strength) than the β relaxation of the polymer and a relaxation time intermediate between those of the α and β relaxations. The presence of two spectral components is visible in the inset of Fig. 3(d), which displays the total fit and fit components (Eq. (1)) for the spectra of the 10 % and 20% ASDs in PDLLA at 298 K. We will refer to this new relaxation as α' relaxation for reasons to be discussed in the following.

Besides these three relaxations (two in the case of PLLA), the CAP dispersions displayed also a local secondary relaxation (spectra not shown) at yet lower temperature than the ones displayed in Fig. 3. Such local relaxation is associated with the relative motion of polar groups of the CAP molecule, as reported (Knapik-Kowalczuk et al., 2018; Rivas et al., 2018) in pure CAP. Following previous work, we refer to this local process as γ relaxation.

Considering that the polymer chains have a significantly higher segmental mobility in the presence of the drug, we may expect a similar plasticizing effect of CAP on their

secondary relaxation motions. While the α relaxation frequency shifts by few orders of magnitude as the weight fraction of drug is varied, the shift in frequency of the secondary β relaxation of the polymer in the glass state is less pronounced in Fig. 3(b), which is partially due to the fact that this secondary relaxation is weaker in intensity and broader in frequency. To further study the dependence of the relaxation processes on sample weight composition, we have analyzed the temperature dependence of the characteristic relaxation time (Eq. 2) and dielectric strength obtained by our fitting procedures. Panels (a) and (b) of Fig. 4 display the so-called relaxation map (logarithm of the relaxation time *vs* inverse temperature) of both PLLA and PDLLA dispersions. The experimental relaxations are neatly grouped in three groups (α, β, γ, from longest to shortest relaxation time) in the case of PLLA dispersions, and four groups (α, α', β, γ) in the case of PDLLA dispersions.

It may be noticed that the secondary β and γ processes display a simply activated behavior characterized by constant slope and thus activation energy E_a. Instead, the structural (segmental) α relaxation displays a characteristic curvature, indicative of an effective activation energy that increases as the temperature is decreased towards the glass transition temperature and often encountered in glass forming liquids and polymers. CAP is observed to have a plasticizing effect not only on the segmental relaxation but also on the secondary relaxation (β) of the polymer, both in terms of a shorter relaxation time (higher characteristic frequency) and of a lower activation energy barrier. As for the α' relaxation visible in the PDLLA dispersions with 10 and 20% weight fraction of CAP,

it is found to have a nontrivial temperature behavior, with a clear cross-over at the glass transition temperature of the dispersions which separates a high-temperature regime with nonzero curvature, and a low-temperature regime with a simply activated behavior whose activation energy displays a discontinuity from the effective activation energy in the high-temperature regime.

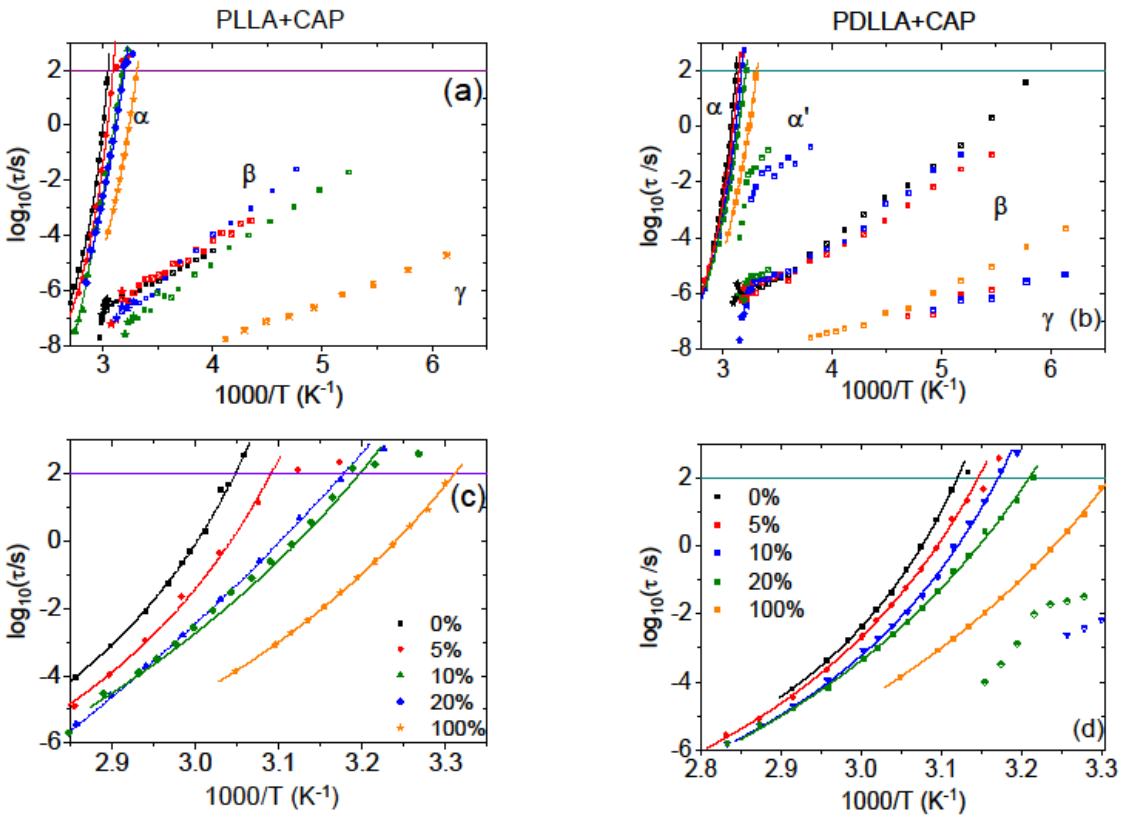

Fig. 4. Relaxation times as function of inverse temperature of all relaxation processes observed in PLLA+CAP (a) and PDLLA+CAP (b) dispersions at different CAP concentrations and in pure CAP (see legends). Open markers represent the β relaxation times, while stars are Coupling Model predictions of the Johari-Goldstein relaxation

times (Eq. 5). Primary (α) relaxation times (filled markers), for PLLA+CAP (c) and PDLLA+CAP (d), and corresponding fits with Eq. 4 (continuous lines).

To better analyze the change of the relaxation dynamics with drug content, in the following we analyze each relaxation in detail, starting from the segmental α relaxation, whose Arrhenius plot is shown separately in panels (c) and (d) of Fig. 4. The dynamic glass transition temperature, defined conventionally as the temperature at which the characteristic time τ_α of the structural relaxation reaches 100 s ($\log(\tau_\alpha) = 2$), and where the viscosity of the dispersion should attain a value of the order of 10^{13} poise, was obtained by fitting the experimental data of τ_α with the Vogel-Fulcher-Tammann (VFT) equation (the typical temperature-dependence of structural processes in glass-forming materials), given by (Böttcher and Bordewijk, 1978):

(4) $$\tau_\alpha(T) = \tau_\infty exp\left(D\frac{T_{VF}}{T-T_{VF}}\right)$$

Here the prefactor τ_∞ represents the high-temperature limit value of the relaxation time, and the "strength parameter" D and the Vogel-Fulcher temperature T_{VF} are phenomenological constants describing the deviation from a simply activated behaviour. Data and fits are shown together in Fig. 4(c) and (d), and the obtained fit parameters are listed in Table 2. These results are interesting also for the rheological properties of the amorphous dispersions, because their viscosity, which is an important parameter for processing purposes (*e.g.* in an extrusion process), is expected to display the same dependence as τ_α on temperature and concentration of the CAP plasticizer.

Table 2. VFT parameters, fragility and activation energies for the relaxations observed in PLLA+CAP mixtures.

CAP w% in PLLA	**$\log_{10}(\tau_0/s)$**	***D***	***T_0* (K)**	***m***	***E_a* (β) (kJ/mol)**
0%	-12.7±0.3	3.7±0.2	289±1	149.2±0.1	42.2±0.6
5%	-13.5±0.6	4.4±0.6	282±3	147±5	46±2
10%	-31±3	48±14	187±14	87.6±0.2	59±9
20%	-17.8±1.7	12±3	240±1	94.8±0.1	51±1

The dielectric T_g values extrapolated from the fit with Eq. 4 are shown in Fig. 2 as a function of the weight fraction of CAP, where they are seen to be in agreement with the calorimetric T_g values and to be well described by the Gordon-Taylor equation (with constants K = 0.18 ± 0.04 for PLLA dispersions and K = 0.16 ± 0.03 for PDLLA dispersions), which confirms the validity of our assignment of this spectral feature. Beside the glass transition temperature, we have also calculated the so-called kinetic fragility index, defined as $m = \left.\frac{d(\log \tau_\alpha)}{d(T_g/T)}\right|_{T=T_g}$, which is a measure of the curvature of the relaxation map of the α relaxation at T_g. The so-obtained fragility indices are listed in Tables 2 and 3 and plotted as insets in Fig. 5(c) and (d), where it is seen that they decrease with increasing drug weight fraction in both polymers (the fragility of pure

amorphous CAP is lower than that of polylactic acid), although the trend is smoother in the case of the dispersions in PDLLA.

Table 3. VFT parameters, fragility and activation energies for the relaxations observed in PDLLA+CAP mixtures and pure CAP.

CAP w% in PDLLA	**α relaxation**				**α' relaxation**			**secondary relaxations**	
	$\log_{10}(\tau_0/s)$	***D***	**T_0 (K)**	***m***	**$\log_{10}(\tau_0/s)$**	***D***	**T_0 (K)**	**E_a (β) (kJ/mol)**	**E_a (γ) (kJ/mol)**
0%	-11.4±0.2	2.8±0.1	294.1±0.6	164±6	-	-	-	58±1	-
5%	-13.0±0.5	4.2±0.4	284±2	139±1	-	-	-	38±1	36±7
10%	-12.6±0.4	3.8±0.3	283±2	127±4	-6.1±0.3	1.9±0.4	248±7	53±3	43±2
20%	-14.5±0.6	6.5±0.7	266±3	114±6	-8.3±0.9	0.6±0.2	298±2	32±3	-
100%	-15.0±0.7	7.6±0.9	253±3	104±5	-	-	-	59.6±0.6	30.4±0.4

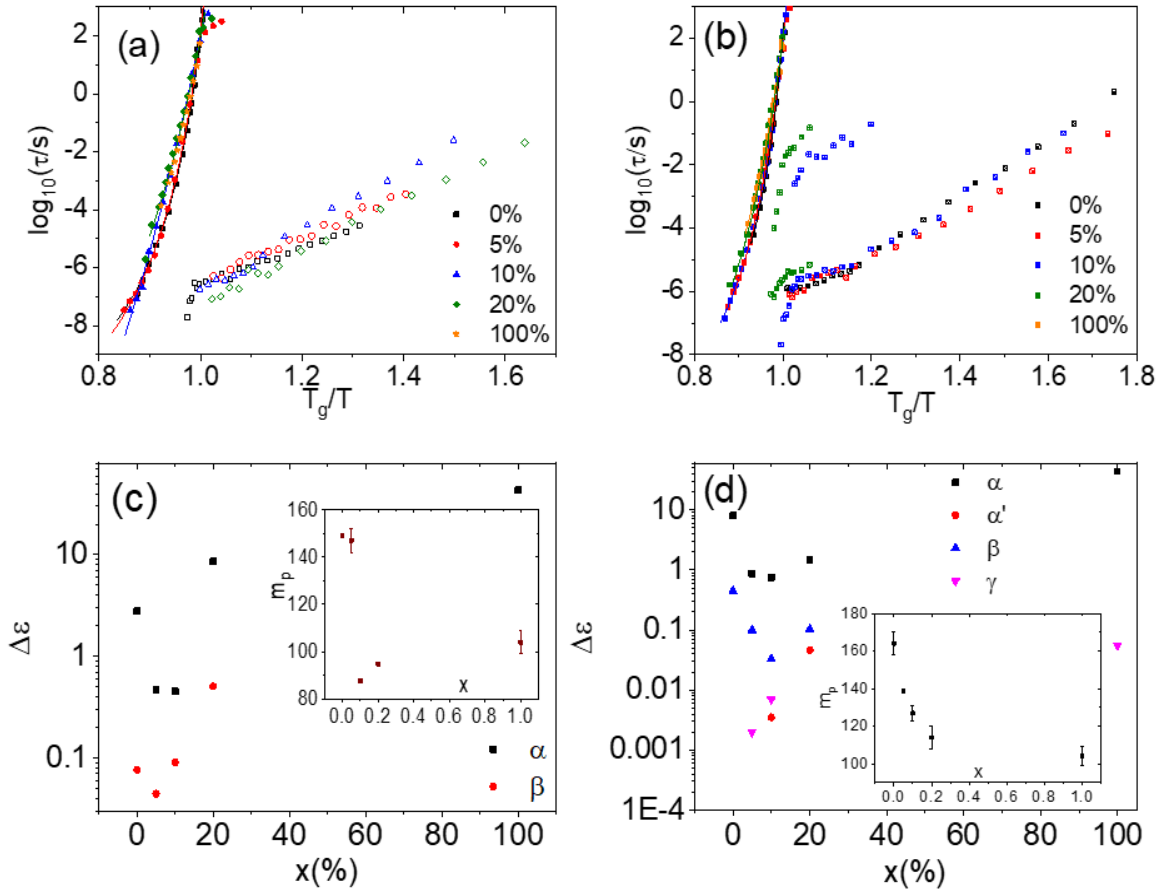

Fig. 5. (a, b) Angell plot of the α (filled markers) and β (open markers) relaxation times of PLLA+CAP and PDLLA+CAP dispersions versus the normalized inverse temperature T_g/T. (c, d) Dielectric strength of all relaxations observed in PLLA+CAP and PDLLA+CAP mixtures, as a function of the drug weight fraction (α, black squares; β, blue triangles; α', red circles; γ, pink triangles). Insets: kinetic fragility index plotted as a function of the drug weight fraction.

Turning now to the other relaxation processes, it is worthwhile to recall that secondary molecular relaxations in glass forming materials may have in general two distinct origins. In some cases, the secondary relaxation corresponds to "intramolecular" motions

involving a relative motion of polar sidegroups of a polymer chain (as in polyvynilpirrolidone (Romanini et al., 2018)) or of a subpart of a molecule (as it is the case for the chloramphenicol molecule (Rivas et al., 2018) and other drugs (Tripathi et al., 2015)). In other cases, the secondary relaxation involves the rigid reorientation of the whole molecule or chain segment, as the cooperative α relaxation but involving only local degrees of freedom (Ngai and Paluch, 2004). The latter secondary relaxations are termed Johari–Goldstein relaxations (Johari and Goldstein, 1970), and they are observed for example in fully rigid molecules (Romanini et al., 2012) and in polymers with monoatomic or methyl sidegroups such as polybutadiene (Schroeder et al., 2007) and 1,4-polyisoprene (Roland et al., 2004), but they are also observed together with intramolecular modes in other polymers (Romanini et al., 2018; Cerveny et al., 2008). The relaxation time of the Johari–Goldstein relaxation usually displays a dynamic crossover at the glass transition temperature T_g.(Kessairi et al., 2008; Ngai and Paluch, 2004; Paluch et al., 2003; Fujima et al., 2002)

At least near the glass transition temperature, the relaxation time of secondary Johari-Goldstein relaxations should be directly correlated with the spectral characteristics of the cooperative α relaxation. In particular, according to the so-called Coupling Model (Ngai, 2007; Ngai, 1998) the relaxation time of Johari–Goldstein relaxations should correspond to a single-molecule precursor time τ_{CM} of the cooperative time τ_α, where τ_{CM} is given by:

(5) $\tau_{\mathrm{CM}} = t_c^{1-n}(\tau_\alpha)^n$.

Here t_c is a universal cross-over time, equal to 2×10^{-12} s for organic (molecular and polymeric) glass formers (Ngai, 1998), and n is equal to the exponent of the stretched Kohlrausch-Williams-Watts (KWW) exponential function that describes the α spectral feature in the time domain. Under most circumstances, the latter can be accurately estimated (Alvarez et al., 1991; Alvarez et al., 1993) from the exponents a and b of the HN fit (Eq. 1) to the α relaxation, as $n \cong (ab)^{\frac{1}{1.23}}$. The predictions of the CM for the Johari–Goldstein relaxation have been verified in some cases of both molecular and polymeric glass formers (Romanini et al., 2012; Schroeder et al., 2007; Johari and Goldstein, 1970).

The theoretical time τ_{CM} estimated using Eq. (5) near the dielectric T_g is shown in panels (a) and (b) of Fig. 4 to allow comparison with the experimental values of the polymer secondary relaxation time τ_β at the same temperatures. It may be observed that while a small discrepancy is found for the pure polymer samples, in all binary dispersions τ_β is virtually identical to the Coupling Model time τ_{CM}. It would thus appear that the secondary process of polylactic acid may have a Johari-Goldstein origin. In previous studies, the secondary relaxation in polylactide acid has been attributed to local chain twisting motions of angular amplitude of the order of 11° (Ren et al., 2003). Our analysis suggests that the β twisting mode of the polymer is the low-cooperativity, local version of the segmental α relaxation associated with the glass transition of the polymer and of the ASDs; this assignment would be consistent with the idea that the JG relaxation

corresponds to a local rigid rotations taking place under strong spatial restrictions (Eisenberg, 1976; Williams and Watts, 1971).

The Angell plot of the α and β relaxations of all polymer samples are shown in panels (a) and (b) of Fig. 5, where it is observed that the β relaxation times are roughly superposed to one another, as expected for a Johari-Goldstein relaxation (Kessairi et al., 2008; Ngai and Paluch, 2004). The dielectric strength of both processes is shown in panels (c,d) of the same figure. The dielectric strength Δε of the Johari-Goldstein process scales with that of the segmental α relaxation, both strengths decreasing with increasing CAP weight fraction. On the other hand, the strength of both the α' and γ relaxations increase with the weight fraction of CAP. This is a clear indication that these processes stem from the CAP molecules in the dispersions. In particular, the similar value of τ_γ in the ASDs compared to that of pure CAP (see Fig. 4(a) and (b)) lead us to conclude that the origin of this relaxation is an intramolecular relaxation of the CAP moieties, which is only barely affected by the molecular environment, as observed also in other drug-polymer mixtures (Romanini et al., 2018).

The assignment of the α' relaxation, which is only observed in PDLLA dispersions with 10 and 20% CAP in weight, is instead less straightforward. It is observed in Fig. 4(b) that the α' relaxation times follow a VFT behavior above the T_g of the dispersion, and that they are shorter than those of the α relaxation of pure CAP. These results suggest that the α' relaxation may be the cooperative relaxation of amorphous CAP domains confined within the polymer matrix. The fact that the ASDs are characterized by a single

calorimetric T_g implies that such domains must have a nanometric size, since for a macroscopic phase separation would result in multiple T_g values. If nanoscopic domains of CAP are formed, their limited size would imply a cooperative rearranging region reduced in size compared with bulk supercooled liquid CAP, which would rationalize the faster dynamics (shorter α' relaxation time) compared to bulk CAP. These domains are only formed in the PDLLA matrix and not in PLLA likely because, the random chirality of the monomers results in a larger free volume between polymer chains that appears sufficient for agglomeration of few CAP molecules (this larger free volume is also responsible for the lower T_g of PDLLA compared to PLLA, as discussed at the beginning of Section 3.1). The cross-over in the temperature behavior of the α' relaxation times visible in Fig.s 4(b) and 5(b) likely reflects the impact, on the structural dynamics of the nano-size CAP domains, of the vitrification of the surrounding PDLLA-CAP matrix.

3.3. Controlled release of CAP from PDLLA dispersions

We have characterized two different ASDs of CAP in PDLLA, with 5 and 20% drug weight fraction, respectively, to study the controlled release of the drug from its carrier in a simulated body fluid (SBF) at human body temperature. The reason for choosing the PDLLA dispersion was that the heating step required to produce fully amorphous ADSs in PLLA likely leads to degradation of CAP; the lower heating temperature in the case of PDLLA ensures on the contrary that no degradation of the antibiotic takes place. The fact that PDLLA dispersion may contain nanoscopic domains of pure CAP does not prevent an effective control of the liberation of this active principle from the polymer matrix, as

we show in the following. The result of the control-release characterization is shown in Fig. 6. The release rate was studied initially in the pure SBF during 70 hours, after which time ethanol was added to the SBF to check that the polymer carrier still contained an appreciable amount of drug at this time. It can indeed be seen that the amount of released drug increases dramatically upon addition of ethanol. The lower value in the pure SBF is due to the fact that the polymer matrix is insoluble in the SBF, so that the drug molecules have to diffuse through it before reaching the solvent, while the sudden surge of the drug concentration in solution (*i.e.*, of the liberation rate) is due to the partial swelling of PDLLA, which exposes the drug directly to ethanol where it is soluble. The different saturation values of the two samples might reflect the presence of nanodomains of pure CAP in the bulk of the 20% sample: these would not contribute to the liberated fraction of the drug at short times in the SBF, while they would be liberated suddenly as the polymer swells in ethanol, which rationalizes the observed difference in percent of liberated drug at long times in the SBF+ethanol mixture.

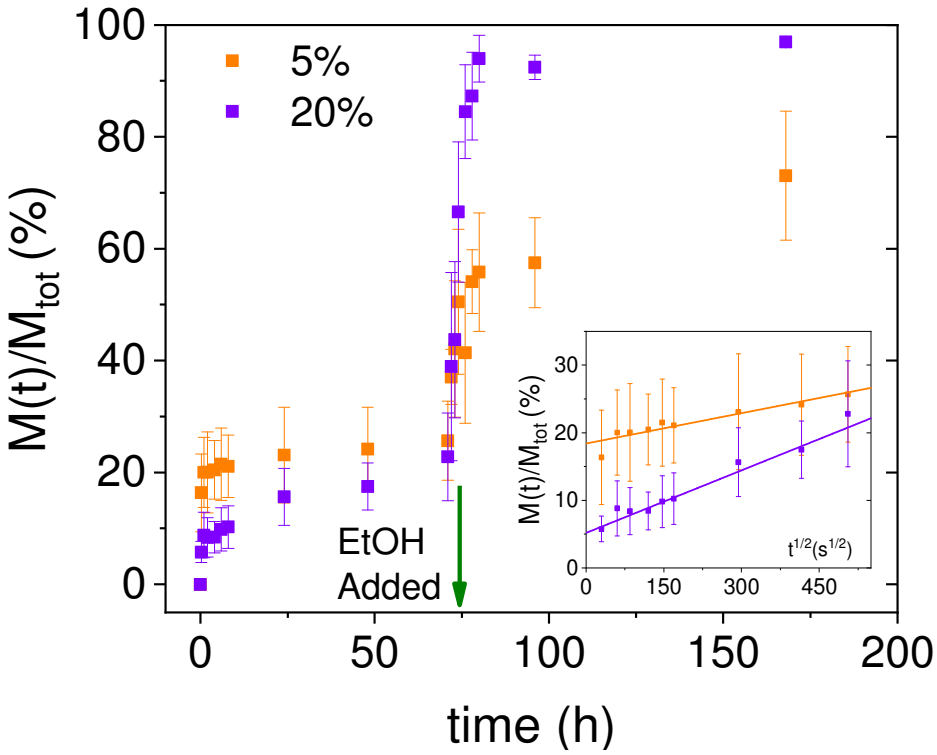

Fig. 6. Release curves for two different PDLLA+CAP ASDs (with 5 and 20% of CAP in weight) in a simulated body fluid (SBF) at human body temperature (310 K), both before and after addition of ethanol in a molar ratio of 3 to 1. Inset: release curves in the SBF (without ethanol), versus the square root of time elapsed since the beginning of the experiment. Markers with error bars are experimental points and continuous lines are linear fits.

It is observed in Fig. 6 that the percent of released drug in the SBF increases quite fast at short times and then reaches a saturation value of about 25% after 70 hours, roughly independent of the initial drug content. The non-zero value of released drug at very short times (less than half an hour from the start of the experiment) is likely due to the presence

of drug molecules/nanodomains at the very surface of the ASD membrane, which is liberated as soon as the membrane is immersed in the SBF.

The inset to Fig. 6 shows that the amount of released CAP is linearly proportional to the square root of time ($t^{1/2}$). This is in agreement with the prediction of simple Fickian diffusion in a thin polymer sample (Siepmann and Peppas, 2011) and with the so-called Higuchi model (Higuchi, 1963). The proportionality constant is 2.1±0.6 10^{-4} $s^{-1/2}$ and 3.1±0.6 10^{-4} $s^{-1/2}$ for the dispersions with 5% and 20% of CAP in weight, respectively. Since in the diffusivity-based models that predict a $t^{1/2}$ dependence the slope is proportional to the square root of the diffusivity D (Siepmann and Peppas, 2011; Higuchi, 1963), the very similar values of the slopes in the inset indicates that the diffusivity of the drug through the polymer is only weakly dependent on the drug content in the ASD, which may be surprising considering that the structural relaxation time τ_α and thus the viscosity are lower by four orders of magnitude in the 20% sample than in the 5% one, due to the increased plasticizer effect (lower glass transition temperature) in the presence of a higher drug content in the dispersion (see Fig.s 2 and 3). In other words, there is no correlation between the release constant and τ_α at 310 K. The fact that the release rate is virtually unchanged even as the drug content decreases by a factor of 4 is particularly interesting for drug release applications, as it entails that roughly the same amount of drug will be liberated per unit time, independent of the drug content of the polymer carrier and thus independent of time elapsed since the beginning of the release.

4. Conclusions

We have characterized the effect of the choice of different polylactic acid polymers (PLLA and PDLLA) as excipients to obtain amorphous solid dispersions of CAP, with the aim of stabilizing the amorphous form of this antibiotic and controlling its release for antitumoral purposes. We have explored thermal as well as dynamical properties of the solid dispersions at different CAP weight fractions by means of calorimetry and dielectric spectroscopy tools. We have observed three (respectively, four) distinct molecular relaxation processes in PLLA (resp. PDLLA), of which the slowest one with longest relaxation times corresponds to the structural relaxation whose freezing marks the glass transition temperature of the dispersion. Although the use of PDLLA avoids a macroscopic phase separation into pure-polymer crystalline domains, the PDLLA dispersions appear to be characterized, at high enough drug loading, by a nanoscopic phase separation into amorphous domains of different chemical composition, namely, amorphous polymer dispersion domains and pure-CAP amorphous nanometric domains. The different sample morphology between the two polymeric forms should have an impact on the kinetic stability of the ASDs, that is, on their tendency to crystallize by phase separation.

We have employed UV/Vis spectroscopy to characterize the release of CAP in a Simulated Body Fluid from PDLLA ADS membranes with 5% and 20% CAP weight fraction. The release takes place over a period of several days, with the released drug fraction being proportional to the square root of time, in agreement with predictions of

Fickian diffusion in a thin polymer sample. The proportionality constant differs by a factor of the order of unity in both ADSs. This similarity of release rate is beneficial as it allows maintaining a steady release rate as the polymer carrier unloads. The drug diffusivity in the ASD appears to be only weakly dependent on drug content, despite the fact that the relaxation time (and the viscosity) of the two samples differ, under the experimental conditions, by as much as four orders of magnitude.

ACKNOWLEDGMENT

This work has been partially supported by the Spanish Ministry of Economy and Competitiveness MINECO through the projects FIS2017-82625-P and MAT2015-69547-R, and by the Generalitat de Catalunya under the project 2017SGR-42.

ABBREVIATIONS

CAP, chloramphenicol; ASD, amorphous solid dispersion; BDS, broadband dielectric Spectroscopy; VFT, Vogel-Fulcher-Tamman; SBF, simulated body fluid.

GRAPHICAL ABSTRACT

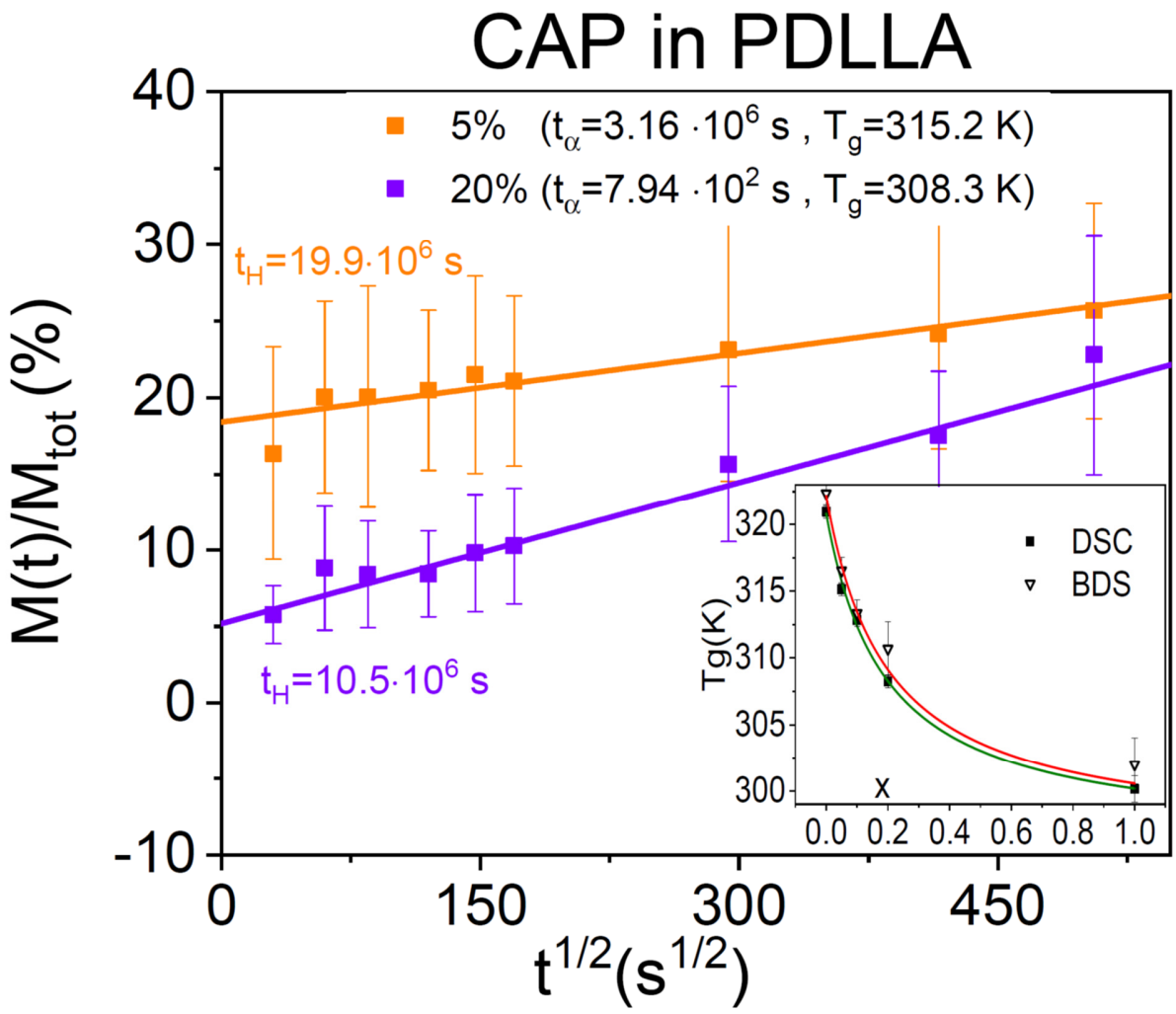

REFERENCES

Abulateefeh, S. R., Alkawareek, M. Y., Alkilany, A. M., 2019. Tunable sustained release drug delivery system based on mononuclear aqueous core-polymer shell microcapsules. Int. J. Pharm. 558, 291-298. https://doi.org/10.1016/j.ijpharm.2019.01.006

Alvarez, F., Alegría, A., Colmenero, J., 1991. Relationship Between the Time-Domain Kohlrausch-Williams-Watts and Frequency-Domain Havriliak-Negami Relaxation Functions. Phys. Rev. B. 44, 7306–7312. https://doi.org/10.1103/PhysRevB.44.7306

Alvarez, F., Alegría, A., Colmenero, J., 1993. Interconnection Between Frequency-Domain Havriliak-Negami and Time-Domain Kohlrausch-Williams-Watts Relaxation Functions. Phys. Rev. B. 47, 125–130. https://doi.org/10.1103/PhysRevB.47.125

Böttcher, C. J. F.; Bordewijk, P., 1978. Theory of electric polarization, Vol. 2, Elsevier Science Ltd.

Bourges, J. L., Gautier, S. E., Delie, F., Bejjani, R. A., Jeanny, J. C., Gurny, R., BenEzra, D., Behar-Cohen, F. F., 2003. Ocular Drug Delivery Targeting the Retina and Retinal Pigment Epithelium Using Polylactide Nanoparticles. Invest. Ophthalmol. Vis. Sci. 44, 3562-3569. https://doi.org/ 10.1167/iovs.02-1068

Cerveny, S., Alegría, A., Colmenero, J., 2008. Broadband Dielectric Investigation on Poly(Vinyl Pyrrolidone) and its Water Mixtures. J. Chem. Phys. 128, 044901. https://doi.org/10.1063/1.2822332

Cole, R. H., Cole, K. S., 1942. Dispersion and Absorption in Dielectrics II. Direct Current Characteristics. J. Chem. Phys. 10, 98. https://doi.org/10.1063/1.1723677

Craig, D., Royall, P., Kett, V., Hoptopn, M., 1999. The Relevance of the Amorphous State to Pharmaceutical Dosage Forms: Glassy Drugs and Freeze Dried Systems. Int. J. Pharm. 179, 179-207. https://doi.org/10.1016/S0378-5173(98)00338-X

Dang, W., Colvin, O. M., Brem, H., Saltzman, W. M., 1994. Covalent coupling of methotrexate to dextran enhances the penetration of cytotoxicity into a tissue-like matrix. Cancer research. 54, 1729-1735.

Davidson, D., Cole, R., 1951. Dielectric Relaxation in Glycerol, Propylene Glycol, and n-Propanol, J. Chem. Phys. 19, 1484. https://doi.org/10.1063/1.1748105

Dedroog, S., Huygens, C., Van den Mooter, G., 2019. Chemically Identical but Physically Different: A Comparison of Spray Drying, Hot Melt Extrusion and Cryo-Milling for the Formulation of High Drug Loaded Amorphous Solid Dispersions of Naproxen. Eur. J. Pharm. Biopharm. 135, 1–12. https://doi.org/10.1016/j.ejpb.2018.12.002

Dorgan, J. R., Janzen, J, Clayton, M. P., Hait, S. B., Knauss, D. M., 2005. Melt Rheology of Variable L-Ccontent Poly(Lactic Acid). J. Rheol. 49, 607. https://doi.org/10.1122/1.1896957

Eisenberg, A., 1976. Discussion in Part III: Secondary Relaxations. Annals of the New York Academy of Science. 279, 141.

Ford, J. L., 1987. The Use of Thermal Analysis in the Study of Solid Dispersions. Drug Dev. Ind. Pharm. 13, 1741-1777. https://doi.org/10.3109/03639048709068690

Fujima, T., Frusawa, H., Ito, K., 2002. Merging of α and slow β relaxation in supercooled liquids. Phys. Rev. E. 66, 031503. https://doi.org/10.1103/PhysRevE.66.031503

Gordon, M., Taylor, J. S., 1952. Ideal Copolymers and the Second-Order Transitions of Synthetic Rubbers. I. Non- Crystalline Copolymers. **J. Appl. Chem.** 2, 493-500. https://doi.org/10.1002/jctb.5010020901

Gupta, P., Chawla, G., Bansal, A., 2004. Physical Stability and Solubility Advantage from Amorphous Celecoxib: the Role of Thermodynamic Quantities and Molecular Mobility. Mol. Pharmaceutics. 1, 406-413. https://doi.org/10.1021/mp049938f

Hancock, B. C., Parks, M., 2000. What Is the True Solubility Advantage for Amorphous Pharmaceuticals? Pharm. Res. 17, 397-404. https://doi.org/10.1023/A:1007516718048

Havriliak, S., Negami, S., 1967. A Complex Plane Representation of Dielectric and Mechanical Relaxation Processes in Some Polymers. Polymer. 8, 161-210. https://doi.org/10.1016/0032-3861(67)90021-3

Higuchi, T., 1963. Mechanism of Sustained-Action Medication: Theoretical Analysis of Rate of Release of Solid Drugs Dispersed in Solid Matrices. J. Pharm. Sci. 52, 1145–1149. https://doi.org/10.1002/jps.2600521210

Jain, D. S., Athawale, R. B., Bajaj, A. N., Shrikhande, S. S., Goel, P. N., Nikam, Y., Gude, R. P., 2013. Poly Lactic Acid (PLA) Nanoparticles Sustain the Cytotoxic Action of Temozolomide in C6 Glioma Cells. Biomed. Aging Pathol. 3, 201-208. https://doi.org/10.1016/j.biomag.2013.08.003

Jelonek, K., Kasperczyk, J., Li, S., Nguyen, T.H.N., Orchel, A., Chodurek, E., Paduszyński, P., Jaworska-Kik, M., Chrobak, E., Bębenek, E., Boryczka, S., 2019. Bioresorbable filomicelles for targeted delivery of betulin derivative–In vitro study. Int. J. Pharm. 557, 43-52. https://doi.org/10.1016/j.ijpharm.2018.12.033

Johari, G. P., Goldstein, M., 1970. Viscous Liquids and the Glass Transition. II. Secondary Relaxations in Glasses of Rigid Molecules. J. Chem. Phys. 53, 2372–2388. https://doi.org/10.1063/1.1674335

Kalaydina, R. V., Bajwa, K., Qorri, B., Decarlo, A., Szewczuk, M. R., 2018. Recent Advances in "Smart" Delivery Systems for Extended Drug Release in Cancer Therapy. Int. J. Nanomed. 13, 4727-4745. https://doi.org/10.2147/IJN.S168053

Kessairi, K., Capaccioli, S., Prevosto, D., Lucchesi, M., Sharifi, S., Rolla, P. A., 2008. Interdependence of Primary and Johari-Goldstein Secondary Relaxations in Glass-Forming Systems. J. Phys. Chem. B. 112, 4470-4473. https://doi.org/10.1021/jp800764w

Knapik-Kowalczuk, J., Wojnarowska, Z., Chmiel, K., Rams-Baron, M., Tajber, L., Paluch, M., 2018. Can Storage Time Improve the Physical Stability of Amorphous Pharmaceuticals with Tautomerization Ability Exposed to Compression? The Case of Chloramphenicol Drug. Mol. Pharmaceutics. 15, 1928−1940. https://doi.org/10.1021/acs.molpharmaceut.8b00099

Kokubo, T., Takadama, H., 2006. How Useful is SBF in Predicting in Vivo Bone Bioactivity? Biomaterials. 27, 2907-2915. https://doi.org/10.1016/j.biomaterials.2006.01.017

Kostopoulou, O. N., Kouvela, E. C., Magoulas, G. E., Garnelis, T., Panagoulias, I., Rodi, M., Papadopoulos, G., Mouzaki, A., Dinos, G. P., Papaioannou, D., Kalpaxis, D. L., 2014. Conjugation with Polyamines Enhances the Antibacterial and Anticancer Activity of Chloramphenicol. Nucleic Acids Research. 42, 8621-8634. https://doi.org/10.1093/nar/gku539

Llorens, E., del Valle, L.J., Díaz, A., Casas, M. T., Puiggalí, J., 2013. Polylactide Nanofibers Loaded with Vitamin B 6 and Polyphenols as Bioactive Platform for Tissue Engineering. Macromol. Res. 21, 775-787. https://doi.org/10.1007/s13233-013-1090-x

Llorens, E., Pérez-Madrigal, M. M., Armelin, E., del Valle, L. J., Puiggalí, J., Alemán, C., 2014. Hybrid Nanofibers from Biodegradable Polylactide and Polythiophene for Scaffolds. RSC Adv. 4, 15245-15255. https://doi.org/10.1039/C3RA42829J

Monro, R. E., Vazquez, D., 1967. Ribosome-Catalysed Peptidyl Transfer: Effects of Some Inhibitors of Protein Synthesis. J. Mol. Biol. 28, 161-165. https://doi.org/10.1016/S0022-2836(67)80085-8

Murdande, S. B., Pikal, M. J., Shanker, R. M., Bogner, R.H., 2011. Aqueous Solubility of Crystalline and Amorphous Drugs: Challenges in Measurement. Pharm. Dev. Technol. 16, 187-200. https://doi.org/10.3109/10837451003774377

Ngai, K. L., 1998. Relation between Some Secondary Relaxations and the α Relaxations in Glass-Forming Materials According to the Coupling Model. J. Chem. Phys. 109, 6982-6994. https://doi.org/10.1063/1.477334

Ngai, K. L., Paluch, M., 2004. Classification of secondary relaxation in glass-formers based on dynamic properties. J. Chem. Phys. 120, 857–873. https://doi.org/10.1063/1.1630295

Ngai, K.L., 2007. Why the Glass Transition Problem Remains Unsolved? J. Non-Cryst. Solids. 353, 709–718. https://doi.org/10.1016/j.jnoncrysol.2006.12.033

O'Neil, M. J. (ed.), 2013. The Merck Index - An Encyclopedia of Chemicals, Drugs, and Biologicals. Cambridge, UK: Royal Society of Chemistry, p. 367.

Paluch, M., Roland, C. M., Pawlus, S., Zioło, J., Ngai K. L., 2003. Does the Arrhenius Temperature Dependence of the Johari-Goldstein Relaxation Persist above Tg? Phys. Rev. Lett. 91, 115701. https://doi.org/10.1103/PhysRevLett.91.115701

Ren, J., Urakawa, O., Adachi, K., 2003. Dielectric and Viscoelastic Studies of Segmental and Normal Mode Relaxations in Undiluted Poly(d,l-lactic acid). Macromolecules. 36, 210-219. https://doi.org/10.1021/ma0212341

Rivas, M., del Valle, L. J., Rodríguez-Rivero, A. M., Turon, P., Puiggalí, J., Alemán, C., 2018. Loading of antibiotic into biocoated hydroxyapatite nanoparticles: Smart antitumor platforms with regulated release. ACS Biomaterials Science & Engineering. 4, 3234-3245. https://doi.org/10.1021/acsbiomaterials.8b00353

Roland, C. M., Schroeder, M. J. Fontanella, J. J., Ngai, K. L., 2004. Evolution of the Dynamics in 1,4-Polyisoprene from a Nearly Constant Loss to a Johari-Goldstein β-Relaxation to the α-Relaxation. Macromolecules. 37, 2630-2635. https://doi.org/10.1021/ma0358071

Romanini, M., Lorente, M., Schammé, B., Delbreilh L., Dupray, V., Coquerel, G., Tamarit, J. Ll., Macovez, R., 2018. Enhancement of the Physical and Chemical Stability of Amorphous Drug–Polymer Mixtures via Cryogenic Comilling. Macromolecules. 51, 9382−9392. https://doi.org/10.1021/acs.macromol.8b01271

Romanini, M., Negrier, Ph., Tamarit, J. Ll., Capaccioli, S., Barrio, M., Pardo, L. C., Mondieig, D., 2012. Emergence of Glassy-Like Dynamics in an Orientationally Ordered Phase. Phys. Rev. B. 85, 134201. https://doi.org/10.1103/PhysRevB.85.134201

Schroeder, M. J., Ngai, K. L., Roland, C. M., 2007. The Nearly Constant Loss, Johari-Goldstein b-Relaxation, and a-Relaxation of 1,4-Polybutadiene. J. Polym. Sci. B Polym. Phys. 45, 342–348. https://doi.org/10.1002/polb.21051

Senapati, S., Mahanta, A. K., Kumar, S., Maiti, P., 2018. Controlled Drug Delivery Vehicles for Cancer Treatment and their Performance. **Signal** Transduct. **Target** Ther. 3, 7. https://doi.org/10.1038/s41392-017-0004-3

Serajuddin, A., 1999. Solid Dispersion of Poorly Water-Soluble Drugs: Early Promises, Subsequent Problems, and Recent Breakthroughs. J. Pharm. Sci. 88, 1058-1066. https://doi.org/10.1021/js9804031

Siepmann, J., Peppas, N. A., 2011. Higuchi Equation: Derivation, Applications, Use and Misuse. Int. J. Pharmaceutics. 418, 6–12. https://doi.org/10.1016/j.ijpharm.2011.03.051

Siepmann, J., Faham, A., Clas, S.-D., Boyd, B. J., Jannin, V., Bernkop-Schnürch, A., Zhao, H., Lecommandoux, S., Evans, J. C., Allen, C., Merkel, O. M., Costabile, G., Alexander, M. R., Wildman, R. D., Roberts, C. J., Leroux, J.-C., 2019. Lipids and Polymers in Pharmaceutical Technology: Lifelong Companions. Int. J. Pharmaceutics. 558, 128–142. https://doi.org/10.1016/j.ijpharm.2018.12.080

Soriano, I., Evora, C., Llabrés, M., 1996. Preparation and evaluation of insulin-loaded poly (DL-lactide) microspheres using an experimental design. Int. J. Pharm. 142, 135-142. https://doi.org/10.1016/0378-5173(96)04648-0

Tian, F., Wang, C., Tang, M., Li, J., Cheng, X., Zhang, S., Li, H., 2016. The Antibiotic Chloramphenicol May be an Effective New Agent for Inhibiting the Growth of Multiple Myeloma. Oncotarget. 7, 51934-51942. https://doi.org/10.18632/oncotarget.10623

Tripathi, P., Romanini, M., Tamarit, J. Ll, Macovez, R., 2015. Collective Relaxation Dynamics and Crystallization Kinetics of the Amorphous Biclotymol Antiseptic. Int. J. Pharmaceutics. 495, 420-427. https://doi.org/10.1016/j.ijpharm.2015.09.012

Valenti, S., Romanini, M., Franco, L., Puiggalí, J., Tamarit, J. L., Macovez, R., 2018. Tuning the Kinetic Stability of the Amorphous Phase of the Chloramphenicol Antibiotic. Mol. Pharmaceutics. 15, 5615−5624. https://doi.org/10.1021/acs.molpharmaceut.8b00786

Williams, H. D., Trevaskis, N. L., Charman, S. A., Shanker, R. M., Charman, W. N., Pouton, C. W., Porter, C. J., 2013. Strategies to Address Low Drug Solubility in Discovery and Development. Pharmacol. Rev. 65, 315-499. https://doi.org/10.1124/pr.112.005660

Williams, G., Watts, D. C., 1971. Molecular Motion in the Glassy State. The Effect of Temperature and Pressure on the Dielectric β Relaxation of Polyvinyl Chloride. Trans. Faraday Soc. 67, 1971–1979. https://doi.org/10.1039/TF9716701971

Zheng, X., Kan, B., Gou, M., Fu, S., Zhang, J., Men, K., Chen, L., Luo, F., Zhao, Y., Zhao, X., Wei, Y., 2010. Preparation of MPEG–PLA nanoparticle for honokiol delivery in vitro. Int. J. Pharm. 386, 262-267. https://doi.org/10.1016/j.ijpharm.2009.11.014